Journal of Metals, Materials and Minerals, Vol. 30, No. 2, pp. 83-90, 2020

Tribology, mechanical properties and coloration of a mica glass-ceramic

Sahadsaya PRASERTWONG[1], Sukanda ANGKULPIPAT[1], Thapanee SRICHUMPONG[1], Kallaya SUPUTTAMONGKOL[2], Chanchana THANACHAYANONT[3], Ramona SOLA[4], Greg HENESS[1,5], Cristina LEONELLI[4], and Duangrudee CHAYSUWAN[1,*]

[1] *Department of Materials Engineering, Faculty of Engineering, Kasetsart University, Bangkok 10900, Thailand*
[2] *Department of Prosthodontics, Faculty of Dentistry, Mahidol University, Bangkok 10400, Thailand*
[3] *National Metal and Materials Technology Center, Thailand Science Park, Pathum Thani 12120, Thailand*
[4] *Department of Engineering "Enzo Ferrari", University of Modena and Reggio Emilia, Modena 41125, Italy*
[5] *UTS Insearch, University of Technology Sydney, PO Box K1085 Haymarket NSW 1240, Australia*

[*]**Corresponding author e-mail:** fengddc@ku.ac.th

Received date:
30 September 2019
Revised date:
23 March 2020
Accepted date:
27 March 2020

Keywords:
Mica glass-ceramic
Nanoindentation
Tribology
Wear
Coloration

Abstract

The research employed pigments, Fe2O3 and CeO2, into the glass frit for adjustable mechanical properties and coloration. Disc samples were prepared to determine microstructures and mechanical properties in terms of tribology and nano-indentation hardness as well as biaxial flexural strength. The glass system presented the crystalline phases, by XRD, of phlogopite Ca-mica, fluorapatite, stishovite, anorthite and strontium apatite. Furthermore, SEM micrographs revealed rod-like microstructures and parent glass phase in all specimens 1) GC, 2) GC + 1wt% CeO_2, 3) GC + 0.1wt% Fe_2O_3 and 4) GC + 1wt% CeO_2 + 0.1wt% Fe_2O_3. For the tribology test, specimens were tested by a pin-on-disc tribometer with 10 N load and 1,000 wear cycles. The obtained values of wear rate and friction coefficient of GCF were better than those of others. The nano-indentation hardness results showed that GC exhibited 3.2 GPa which lower than those of GCC, GCF and GCCF, respectively. The addition of pigments affected reddish yellow color. After crystallization, the contrast ratio is around 0.72 for GC and decreases to 58-75% for the mica glass-ceramics that contain the pigments. The values of biaxial flexural strength of all were acceptable (≥100 MPa) according to ISO 6872:2015.

1. Introduction

Brittle enamel coat is probably damaged by the living activity e.g. chewing. This can be the cause of suffered oral health. Dental prostheses play an important role for the restoration of decayed teeth [1-5].

Glass-ceramics are considered highly suitable materials for restorative dental materials because of their high strength, high wear resistance, machinability and esthetics [6]. The properties of glass-ceramics are controlled by the heat treatment process of the glass. The heat treatment involved two-stage process, called nucleation and crystallization. One of glass-ceramics used today is mica-based glass-ceramics which contain the glassy and crystalline phases to result in the effective toughening and reinforcing. The microstructure of mica glass-ceramics consists of randomly oriented plate-like crystals which are important features to make them machinable and deflecting cracks in the glass matrix [7]. For improvement of the properties of glass-ceramics, some additives are needed. Sun *et al.* [8,9] found that adding CeO_2 and Fe_2O_3 to glass-ceramics as pigments to improve their coloration and appearance because the crystals of the pigments are incorporated into the composition. However, several studies have been reported on the failure of ceramic restoration caused by the wear during the mastication in the mouth [1,10]. The wear is usually the cause of slow removal of materials due to their interaction between surfaces moving in contact [11,12]. The reliability of the biomedical mainly depends on their fracture and tribological behaviors. It is essential to evaluate the tribological behaviors of implants and dental materials, because they are often subjected to wear debris and surface degradation while in direct contact with host tissues. A systematic of tribological behaviors, such as friction and wear of biomaterials is therefore of great importance, which helps predict the reliability and long-term performance of the dental materials in the oral environment [13]. Therefore, wear resistance of different kind of glass ceramics should be evaluated by the perspective of the progressive wear behaviors.

Prior to the study on the properties of wear resistance of the glass-ceramics, the research was conducted in the laboratory and found that the phlogopite Ca-mica and fluorapatite glass-ceramic could be used as restorative dental materials because the previous researches reported that the glass-ceramics containing 3.5 mol% fluorapatite increased both strength (101.5-115.2 MPa) and fracture toughness (1.36 - 2.04 $MPa \cdot m^{1/2}$) [14,15] reaching the standard requirement according to ISO 6872:2015. However, the color of the mica-glass-ceramics in previous research were white and relatively opaque which need to be improved in the color aspect for the appearance similar

DOI: 10.14456/jmmm.2020.24

to human teeth. The aim of this study was to evaluate the color improvement of mica glass-ceramics by adding CeO_2 and Fe_2O_3. Additionally, wear mechanism, mechanical properties such as the biaxial flexural strength, Young's modulus and nano-indentation hardness were investigated.

2. Experiment

2.1 Glass-ceramic specimens preparation

Mica-based glass-ceramics systems were made from feedstocks of SiO_2-Al_2O_3-MgO-MgF_2-$SrCO_3$-$CaCO_3$-CaF_2-P_2O_5. The various amounts of pigments were added into the glass frit. Four different formulae of mica-based glass-ceramics were prepared in this research as shown in Table 1. For the glass frit preparation, all materials were mixed for 2 h and placed in an alumina crucible prior to melt in the furnace at 1420°C for 1 h with heating rate of 10°C·min^{-1}, then quenched into water. Glass frit were ground to obtain glass powder (<45 μm) by high speed planetary ball mill. After that, Fe_2O_3 (Sigma-Aldrich, USA) and/or CeO2 (Sigma-Aldrich, Germany) were added into the glass powder. The glass powder was remelted and poured into a carbon mold. The glass specimens were annealed at 582°C for 1 h 30 min to release stress concentration. Subsequently, the specimens were heat-treated with heating rate of 55°C·min^{-1} for nucleation and crystallization at 643°C and 897°C, respectively, for 10 min in each process to obtain glass-ceramics.

Table 1. Glass-ceramics conditions by weight percent (wt%).

Specimens Code	Glass frit (wt%)	Fe_2O_3 (wt%)	CeO_2 (wt%)
GC	100.0	-	-
GCF	99.9	0.1	-
GCC	99.0	-	1.0
GCCF	98.9	0.1	1.0

2.2 X-ray diffraction analysis (XRD)

All glass-ceramic samples were ground to powder (<45 μm) and XRD characterization were performed by X'Pert Pro diffractometer (PW 3050/60, PANalytical) using Ni filtered Cu Kα_1 radiation. The diffraction patterns were recorded in the 2θ range from 10° to 80° and phases were identified by JCPDS numbers.

2.3 Scanning electron microscope (SEM)

All glass-ceramic specimens were polished and etched using 10% hydrofluoric acid for 15 s, followed by distilled water rinse to remove debris and gold sputtering. The microstructural characteristics, for example, crystalline structure of glass-ceramic were observed using a scanning electron microscope (Quanta 450, FEI Company, USA). For the qualitative characterization of wear tracks after wear testing of glass-ceramic, the worn surfaces of specimens were gold sputtered then, examined using a scanning electron microscope (Quanta 200 ESEM FEG, FEI Company, USA). The damage on the glass-ceramic surfaces, caused by wear tests, was characterized to reveals the propagation of wear crack on surfaces.

2.4 Tribological test

In order to obtain glass-ceramics specimens for the wear test, the specimens were embedded and cold mounted with resin in the middle of a mold to be disc-shaped specimens. The disc specimens were rubbed in a two-body pin-on-disc wear testing machine (CSM Instruments, Needham, Massachusetts, USA) against by 6.0 mm diameter alumina counter body. A total load of 10 N was applied at the end of lever arm with the speed of 200 rpm. The complete distance of 31.39 m was attained by rubbing the pins for 300 s to meet a considerable wear. All set of experiments were repeated in exactly the same method and the precise value was taken for calculating the specific wear rate. Consequently, the substance loss of specimen surfaces was measured using a confocal scanning optical microscope (Eclipse LV150N, Nikon, NY, U.S.A.) with the dedicated software (ConfoViz2, ConfoVis GmbH, Jena, Germany). The wear volume of the specimen calculated by measuring the average worn area of each track on the disc following the wear test from the profiles recorded at three different locations across the wear track, and then multiplying the cross-sectional area of each track [16]. The specific wear rate (W) with the unit of mm^3·N^{-1}m^{-1} can be calculated with the following equation (1)

$$W=\frac{V}{PL} \quad (1)$$

Where P is the normal applied load in N and L is the total sliding distance in m and V is the calculated wear volume.

The friction coefficient (K) is widely used as an index of wear severity. The friction coefficient was calculated by dividing the wear volume by the load and sliding distance, and normalising with respect to the hardness.

$$K=\frac{VH}{PL} \quad (2)$$

Where V is the wear volume, L is the sliding distance, P is the applied load and H is the hardness.

2.5 Nano-indentation hardness

The nano-indentation hardness was carried out using a 3-sided pyramidal Berkovich (142.3-degree diamond probe) fitted in the micro-combi tester

(Micro-combi tester, CSM Instruments, Needham, Massachusetts, USA). The indentation was achieved using a load of 200 mN. At least 100 indentations were obtained to plot the precise loading-unloading curves of the nano-indentation hardness and Young's modulus. The test was made in a room atmosphere and at a constant loading. The indentation load-displacement data were calculated for the absolute hardness (*H*) and Young's modulus (*E*) according to the method of Oliver and Pharr [17]. The Young's modulus was calculated from the equation (3):

$$\frac{1}{E_r}+\frac{(1-v_s^2)}{E_s}=\frac{(1-v_i^2)}{E_i} \quad (3)$$

Where E_r is the reduced modulus; Es is the Young's modulus of the specimens; E_i is Young's modulus of the indenter; ν_s and ν_i are the Poisson's ratio of the specimen and the indenter; respectively.

Nano-indentation hardness is defined as the maximum load, P_{max}, divided by the projected area of the contact impression, A, as the equation (4)

$$H=\frac{P_{max}}{A} \quad (4)$$

2.6 Biaxial flexural strength

The biaxial flexural strength test was performed with piston on three balls to determine the strength of specimens with four formulae of glass-ceramics. The specimen was a disc of 15 mm diameter and 2 mm thickness of each glass-ceramic following ISO 6872:2015. Each specimen was supported on three stainless steel balls, 3.17 mm diameter and positioned 120° apart on a circle 10 mm diameter platform. The specimens were tested at room temperature and loaded using a universal testing machine (Instron®5566, USA) at a crosshead speed of 0.5 mm min^{-1} until failure. The biaxial flexural strength was calculated according to the equation (5).

$$\sigma = -0.2387\frac{P(X-Y)}{b^2} \quad (5)$$

When $X=(1+v)\ln(\frac{r_2}{r_3})^2+[\frac{1-v}{2}](\frac{r_2}{r_3})^2$,

$$Y=(1+v)[1+\ln(\frac{r_1}{r_3})^2]+(1-v)(\frac{r_1}{r_3})^2$$

Where σ is the maximum center tensile stress (MPa), P is the load causing fracture (N), b is the specimen thickness at fracture origin (mm), ν is Poisson's ratio (of ceramic = 0.25, ISO 6872), r_1 is the radius of support circle (1.6 mm), r_2 is the radius of loaded area (0.8 mm) and r_3 is the radius of a specimen (7.8 mm).

2.7 Coloration

The optical properties of glass-ceramics were determined using spectrophotometer (Colorflex 45/0, Hunter Lab, Reston, VA, USA) to acquire the translucency parameter (TP) and contrast ratio (CR) for translucency evaluation with reading ranging from 400 nm to 700 nm, observation angle 10° and D65 illuminant. The specimens were cut at 1.0 mm thickness and finished polished with a grinder polisher. The color of specimens were measured according to the CIE L*a*b* color scale over white and a black background to obtain L*a*b* values that were calculated the translucency parameter (TP) value.

3. Results and discussion

3.1 X-ray diffraction

X-ray diffraction patterns presented phlogopite-Ca mica ($CaMg_6Al_2Si_6O_{20}F_4$, JCPDs : 00-025-0155), fluorapatite ($Ca_5(PO_4)_3F$, JCPDs : 00-060-0667) and stishovite (SiO_2, JCPDs : 00-015-0026), strontium apatite ($Ca_5(PO_4)_3Sr$, JCPDs : 01-077-9725), strontium aluminium silicate ($SrAl_2Si_2O_8$, JCPDs : 00-014-0588), anorthite ($CaAl_2Si_2O_8$, JCPDs : 01-075-1587) phases for all formulae (Figure 1). The diffraction peaks with relatively strong intensities could be indexed as phlogopite-Ca mica and fluorapatite at approximately 28° and 33° 2θ, respectively. It is obviously seen that hump peaks occur at 10-20° 2θ with adding cerium oxide in both GCC and GCCF. When comparing all current XRD patterns with and without adding pigments, it was seen that the pigments of CeO_2 and Fe_2O_3 did not affect the type of crystals.

3.2 Scanning electron microscope

The representative SEM micrographs of fracture surfaces of specimens with added pigments are shown in Figure 2 (1a-1d). For mica glass-ceramics, the plate-like structure sheets of crystals were clearly observed and they were surrounded by the parent glass, which can be machined by the dental CAD/CAM milling machine. Figure 2 (2a-2d) showed that glass-ceramics has a dense with heterogenous microstructures consisting of rod-like crystals randomly distributed throughout the glass matrix. When metal oxides were added, the crystalline appearance presents a bit change with less aspect ratio, for example, the rod-like crystals of GCC and GCCF (Figure 2 (2c-2d)) are seen with significantly larger expansion. Furthermore, there are more glassy phase in both glass-ceramics than others in which confirmed by XRD patterns in Figure 1. However, it shows more crystalline phases in Figure 2 (2b) which may cause for the better wear behavior. The pigments added did not affect the type of crystals because no apparent differences among the crystals grown in the glass-ceramics.

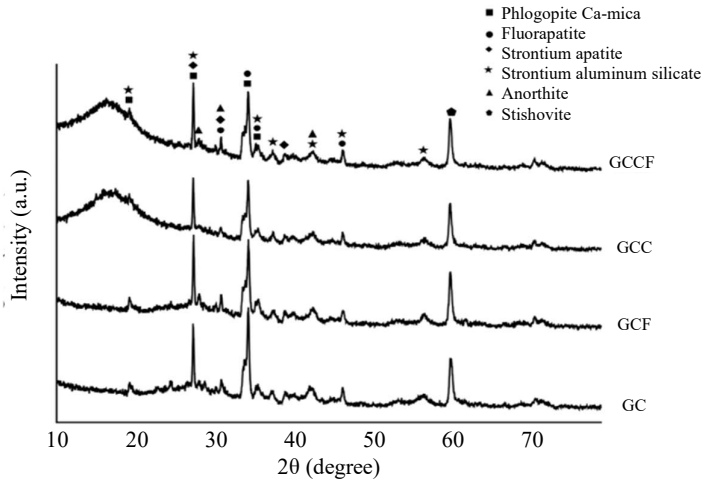

Figure 1. X-ray diffraction patterns of the various glass-ceramics.

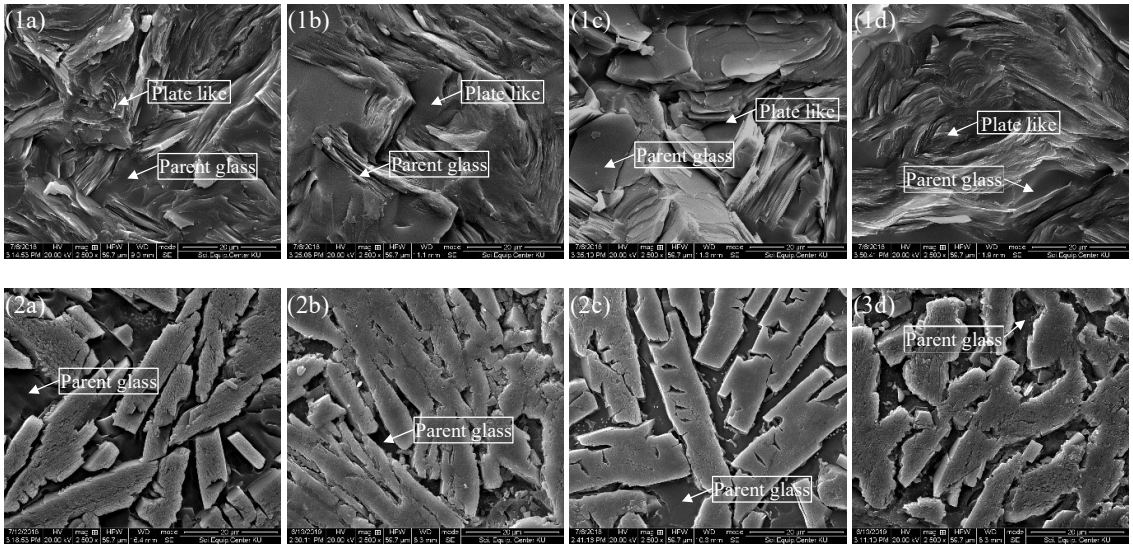

Figure 2. The microstructure of glass-ceramic (a) GC, (b) GCF, (c) GCC and (d) GCCF, x2500.

3.3 Tribology

The values for surface roughness (Sa), wear volume, wear rate and friction coefficient determined from the tracks of worn surfaces are shown in Table 2. The surface roughness of all specimens was automatically reported as arithmetic mean roughness determining in the same reference length of diagonal. The results were between 1.01 to 1.59 that had not much difference on the glass-ceramics surfaces despite of pigments addition in matrix. For wear volume of all specimens, GCC possessed the highest value of 1.449 mm^3 and GCF exhibited the lowest value of 0.0481 mm^3. During experiment, the temperature may increased with increase in sliding distance. It was found that the softened surfaces got more easily separated from the surface of the samples, and as a result, the wear volume of GCC had the highest when compared with others specimens. It implies that CeO_2 may induce more glassy phase in the glass-ceramic and cause the more wear volume in both GCC and GCCF whereas Fe_2O_3 affects in term of wear resistance in this glass-ceramic system.

The wear mechanism of glass-ceramics depends on the nature of materials, bite force, tribology and clinical factor [18,19]. In general, the wear rate of restorative dental materials should be similar to human enamel [20] because the enamel was in contact and friction with others. The wear rate results were observed that the Fe_2O_3 addition reduced of mica-glass ceramics by GCF has the highest wear resistance (0.00155 $mm^3 \cdot N^{-1}m^{-1}$). The low wear rate observed in this study may be attributed to the presence of the hard Fe ions in the matrix. Whereas the CeO_2 addition gradually increased the wear rate, GCC had the highest value of 0.00467 $mm^3 \cdot N^{-1}m^{-1}$. However, when compared the wear rate of a commercial mica-containing glass-ceramic (Dicor®) designed for use as restorative dental materials and GCF; it was found that the wear rate of

GCF (1.5×10^{-3} $mm^3 \cdot N^{-1}m^{-1}$) was lower than that of Dicor® (2.6×10^{-3} $mm^3 \cdot N^{-1}m^{-1}$) [1]. Results revealed that wear resistance of glass-ceramics has been enhanced through the improvement by Fe_2O_3 addition. However, the wear rate of specimens may increase due to occurrence of thermal softening. The surfaces of the sample which had become more softened attaining more depth. The higher surface roughness of surfaces generally results in lower wear resistance.

The friction coefficient typically depends upon the surface conditions of the materials. It presents that the average friction coefficient of samples is very similar. The friction coefficient of GC, GCF, GCC and GCCF were 0.78, 0.76, 0.74 and 0.74, respectively. The wear debris generated due to rubbing in between the contact surfaces also has been found to play a significant part. A decrease in friction coefficient was observed when added Fe_2O_3 into the glass-ceramics. The low friction coefficient in turn leads to low abrasion wear of glass-ceramics and good clinical performance [21]. The effect of pigments on the friction coefficient does not relate significantly to the glass-ceramic system. It should be noted that it is not possible to determine more accurate values of the friction coefficient due to changes in the surface conditions of the dental materials. There are several factors affecting the true frictional values of the biomaterials. For instance, surface layer conditions, such as surface contamination, surface coating, surface roughness, load, sliding velocity, temperature and lubricants, are greatly influencing frictional values and thus they are critical when measuring friction.

All the worn surfaces were studied by FESEM analysis primarily to understand and get insights into the process of wear. FESEM micrographs are shown in Figure 3. Observation of the wear of surface of GCF using an FESEM reveals the cracks. Using SEM images, it is possible to identify wear mechanism that operate under two-body abrasive process. The sliding scratches can be observed on the glass-ceramic samples, being attributed to the abrasive wear caused by the transferred material to the alumina ball. The images of wear scar indicated a smooth surface without any cracks. Mostly oriented grooves parallel to the sliding direction are observed on all samples wear surfaces. Also, it can be noticed cracks through the wear track, which is typical wear feature of the glass-ceramics as they are brittle, and the wear of their surface occurs by fracture [22]. The wider wear track area is detected for GCC confirmed a surface damage acceleration relative to the other samples. The wear particles as fine particles from surfaces of GCC, probably, cause wider wear tracks of GCC, due to the repeated sliding and relatively higher stress close to surface. These relatively large wear track is likely generate large wear particles from delamination which results a high wear rate [23].

Cracks are observed on the worn surface of GCF because while sliding loads against surfaces, then the sliding contact forms plastically deformed regions and initiates micro-cracks, propagating under cyclic loadings. It can be noticed cracks through the wear track which is typical wear feature of the glass-ceramics as they are brittle, and the wear of their surface occurs by fractures [24]. It is concluded that wear primarily occurs by a micro fracture process along the mica glass-ceramic interfaces [5].

Table 2. Wear parameters for mica glass-ceramics.

Specimens Code	Surface roughness, R_a (nm)	Wear volume (mm^3)	Wear rate ($mm^3 \cdot N^{-1}m^{-1}$)	Friction coefficient
GC	1.12 (±0.06)	0.0810	0.00262	0.78 (±0.07)
GCF	1.13 (±0.12)	0.0481	0.00155	0.76 (±0.11)
GCC	1.18 (±0.06)	1.4486	0.00467	0.74 (±0.10)
GCCF	1.38 (±0.21)	1.0019	0.00323	0.74 (±0.04)
Enamel	1.6 ± 0.4	-	-	-

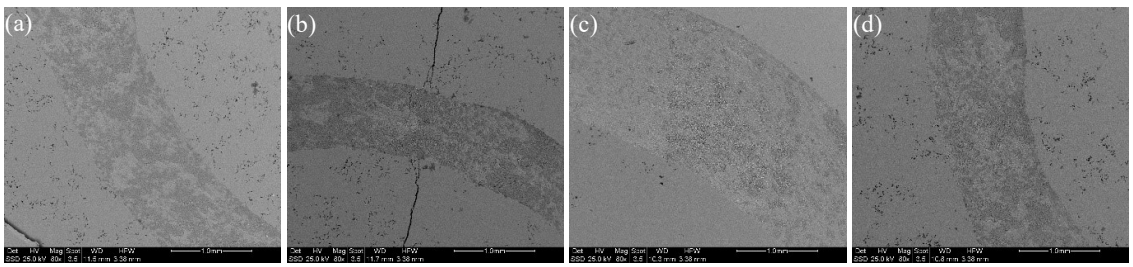

Figure 3. Worn areas of tracks on disc of glass-ceramics by FESEM (a) GC, (b) GCF, (c) GCC and (d) GCCF, x160.

3.4 Mechanical properties

The mechanical properties such as nano-indentation hardness, biaxial flexural strength and Young's modulus of glass-ceramic and those of commercial glass-ceramics are shown in Table 3. The nano-indentation hardness of GC had the lowest hardness that was 3.2 GPa. It slightly increased by adding a small content of pigments, especially GCF had the highest values. It was abundant proportion of glassy phase that had higher hardness than that of crystalline phase, therefore, GCF had probably higher wear resistance than others. When compared the hardness of all specimens with human teeth, it was found that the hardness of all specimens was nearly similar to human enamel but lower than that of a commercial glass-ceramic [26]. For dental ceramics with higher hardness, excessive wear of opposing natural teeth is a major concern because these ceramics would be come into contact with dentin and enamel inevitably during function or parafunction. Materials with low hardness would be more preferable in this case. For biaxial flexural strength, it gives no significant differences between GC and pigments added mica glass-ceramics (GCC, GCF and GCCF). The BFS was in range of 100.2 MPa to 106.8 MPa. However, the BFS values of all specimens was accepted according to standard of ISO 6872:2015 [25] for use as restorative dental materials. It can be used as a body ceramic directly contact with oral environment as partially or fully covered substructure ceramic for single-unit anterior or posterior prostheses adhesively cemented. As regards the Young's modulus results, it shows that value of GCCF presents the highest and more than that of Vita Zahnfabrik [17]. However, it is believed that the hardness is considerably important to the enamel of natural teeth [26].

3.5 Colorimeter

In order to produce acceptable colors for using restorative dental applications, thus, mica glass-ceramics should be yellow to reddish yellow gradient in products. The representative of specimens are shown in Figure 4 which is controlled pigments factor. CeO_2 and Fe_2O_3 and CeO_2-Fe_2O pigments could be used for shade adjusting of mica glass-ceramics without any significant effect on type of crystals. The combination of CeO_2 and Fe_2O_3 of mica glass-ceramics also produced a reddish yellow color and increase the translucency. Color of materials is scientifically defined by a three variables/dimensions of color are value/ lightness, chroma and hue that can be specified CIE Lab color space. The difference CIE color space of specimens tested with white and black backgrounds was calculated TP value. Table 3 presents results of TP and CR by they are general factors to translucency evaluation. From the results, it was found that the pigments addition affected to the optical properties of mica glass-ceramics to more translucency because CR decreased to be closed to 0. The ranges for CIE L*, a* and b* as shown in Table 4 were -10.6 to -16.3, -0.51 to -2.2, and -0.1 to 7.3, respectively. The translucency parameter (TP) were 10.7 to 27.6 and similar to that of commercial restorative dental materials, e.g., Lava Zirconia and IPS e.maxPress HT A1. The opacity has been affected to the particle size and uniform dispersion that increase as the number of reflecting particles per unit volume increase. Table 5 presents TP and CR values of specimens. The TP values had lower than that of dentin and enamel (18.1) Moreover, the pig-ments addition increased a translucency of glass-ceramics as well as color appearance by reducing CR around 58-72% from GC's CR value.

Table 3. Mechanical properties our glass-ceramics.

Groups	Nanoindentation hardness (GPa)	Young's Modulus (GPa)	Biaxial flexural strength (MPa)
GC	3.2	62.5	105.2
GCF	3.6	68.8	106.8
GCC	3.3	71.4	105.2
GCCF	3.6	79.3	100.2
Vita Zahnfabrik [18]	5.8	72	120
IPS e.max CAD [18]	5.8	105	488
human enamel [26]	3.2	94	280
Limit of ISO 6872 (ISO, 2015)			
• Class 1	-	-	≥ 50
• Class 2	-	-	≥ 100

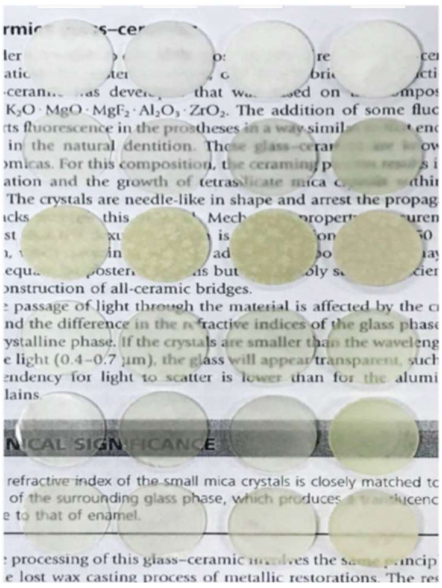

Figure 4. Appearance of glass-ceramics.

Table 4. ΔL*, Δa* and Δb* values of glass-ceramics.

Materials	ΔL*	Δa*	Δb*
GC	-10.64	-0.536	-0.138
GCF	-16.294	-0.508	3.832
GCC	-14.093	-2.189	7.309
GCCF	-10.795	-1.022	4.432

Table 5. CR and TP mean values of glass-ceramics.

Materials	CR Mean	TP Mean
GC	0.72 (±0.03)	10.66 (±0.68)
GCF	0.18 (±0.08)	16.75 (±0.26)
GCC	0.30 (±0.05)	15.28 (±0.56)
GCCF	0.27 (±0.08)	11.71 (±0.44)
IPS e.maxPress HT A1	0.37 (±0.02)	26.59 (±0.83)
IPS Empress Esthetic	0.34 (±0.01)	27.64 (±0.42)
Lava Zirconia	0.73 (±0.01)	10.43 (±0.14)

4. Conclusions

The results showed that CeO_2 and Fe_2O_3 as pigments had a positive effect on the coloration. It could be concluded that the addition of pigments to the mica glass-ceramics giving the expected results of heat-treated samples for translucency and coloration. Results of the color analysis show that the addition of pigments in mica glass-ceramics improved the clinical shade of the glass-ceramics to close to that of natural teeth for more esthetic. It has been observed that Fe_2O_3 in GCF is an effective agent for reduced wear rate compared to other samples. It was found that the coefficient of friction decreased with added pigments. This study is in agreement with the findings of other studies that reported no significant improvement on hardness values by the addition of pigments to glass-ceramic. All materials in this study possess biaxial flexural strength values passing the standard of ISO 6872:2015 for dental ceramics to be used as core materials.

5. Acknowledgements

The authors would like to thank Kasetsart University Research and Development Institute (KURDI) and Faculty of Engineering, Kasetsart University for research funds, scholarship and workplaces. In addition, we also thank Department of Engineering "Enzo Ferrari", University of Modena and Reggio Emilia, Department of Prosthodontics, Faculty of Dentistry, Mahidol University and National Metal and Materials Technology Center, Thailand Science Park for the provision of the analytical equipments and laboratory spaces as well as their support in this research.

References

[1] J. Park and A. Ozturk, "Tribological properties of MgO–CaO–SiO_2–P_2O_5–F-based glass-ceramic for dental application," *Materials letters,* vol. 61, pp. 1916-1921, 2007.

[2] F. Santos, A. Branco, M. Polido, A. P. Serro, and C. G. F.-Pina, "Comparative study of the wear of the pair human teeth/Vita Enamic® vs commonly used dental ceramics through chewing simulation," *Journal of the Mechanical Behavior of Biomedical Materials*, vol. 88, pp. 251-260, 2018.

[3] Z. M. Jin, J. Zheng, W. Li, and Z. R. Zhou, "Tribology of medical devices," *Biosurface and Biotribology*, vol. 2, pp. 173-192, 2016.

[4] V. S. Nagarajan and S. Jahanmir, "The relationship between microstructure and wear of mica-containing glass-ceramics," *Wear,* vol. 200, pp. 176-185, 1996.

[5] J. J. Kruzic, J. A. Arsecularatne, C. B. Tanaka, M. J. Hoffman, and P. F. Cesar, "Recent advances in understanding the fatigue and wear behavior of dental composites and ceramics," *Journal of the Mechanical Behavior of Biomedical Materials,* vol. 88, pp. 504-533, 2018.

[6] A. R. Molla and B. Basu, "Microstructure, mechanical, and in vitro properties of mica-glass-ceramics with varying fluorine content," *Journal of Materials Science: Materials in Medicine,* vol. 20, pp. 869-882, 2009.

[7] D. P. Mukherjee and S. K. Das, "Synthesis and characterization of machinable glass-ceramics added with B_2O_3," *Ceramics International,* vol. 40, pp. 12459-12470, 2014.

[8] Y. Sun, Z. Wang, J. Tian, and X. Cao, "Coloration of mica glass-ceramic for use in

dental CAD/CAM system," *Materials letters,* vol. 57, pp. 425-428, 2002.

[9] L. Holz, J. Macias, N. Vitorino, A. J. S. Fernandes, F. M. Costa, and M. M. Almeida, "Effect of Fe_2O_3 doping on colour and mechanical properties of Y-TZP ceramics," *Ceramics International,* vol. 44, pp. 17962-17971, 2018.

[10] J. Zheng, Y. Zeng, J. Wen, L. Zheng, and Z. Zhou, "Impact wear behavior of human tooth enamel under simulated chewing conditions," *Journal of the Mechanical Behavior of Biomedical Materials,* vol. 62, pp. 119-127, 2016.

[11] Z. R. Zhou, and Z. M. Jin, "Biotribology: Recent progresses and future perspectives," *Biosurface and Biotribology,* vol. 1, pp. 3-24, 2015.

[12] E. d' Incau and P. Saulue, "Understanding dental wear," *Journal of Dentofacial Anomalies Orthodontics,* vol. 15, pp. 1-19, 2012.

[13] V. Preis, S. Hahnel, M. Behr, and M. Rosentritt, "Contact wear of artificial denture teeth," *Journal of Prosthodontics Research,* vol. 62, pp. 252-257, 2018.

[14] T. Srichumpong, K. Suputtamongkol, W. Chinpanuwat, P. Nampachoke, J. Bai, S. Angkulpipat, S. Prasertwong, and D. Chaysuwan, "Effect of Heat Treatment Time on Properties of Mica-Based Glass- Ceramics for Restorative Dental Materials" *Key Engineering Materials,* vol. 702, pp. 23-27, 2016.

[15] D. Chaysuwan, K. Sirinukunwattana, K. Suputtamongkol, K. Kanchanatawewat, G. Heness, and K. Yamashita, "Machinable glass-ceramics forming as a restorative dental material," *Dental Materials Journal,* vol. 30, pp. 358-367, 2011.

[16] A. C. Fischer-Cripps, "2-Nanoindentation Testing," in *Handbook of Nanoindentation*, ed Australia: Londonderry Drive 29 Fischer-Cripps Laboratories Pty Ltd., 2011, pp. 21-37.

[17] O. Borrero-Lopez, F. Guiderteau, Y. Zhang, and B. R. Lawn, "Wear of ceramic-based dental materials," *Journal of the Mechanical Behavior of Biomedical Materials,* vol. 92, pp. 144-151. 2019.

[18] V. Preis, M. Behr, G. Handel, S. Schneider-Feyer, S. Hahnel and M. Rosentritt, "Wear performance of dental ceramics after grinding and polishing treatments," *Journal of the Mechanical Behavior of Biomedical Materials,* vol. 10, pp. 13-22, 2012.

[19] C. D'Arcangelo, L. Vanini, G. D. Rondoni, and F. D. Angelis, "Wear properties of dental ceramics and porcelains compared with human enamel," *The Journal of Prosthetic Dentistry*, vol. 115, pp. 350-355, 2016.

[20] Z. Hao, D., H. Yin, L. Wang, and Y. Meng, "Wear behavior of seven artificial resin teeth assessed with three-dimensional measurements," *The Journal of Prosthetic Dentistry,* vol. 112, pp. 1507-1512, 2014.

[21] R. L. P. Santos, M. Bucimeaunu, F. S. Silva, J. C. M. Souza, R. M. Nascimento, F. V. Motta, O. Carvalho, and B. Henriques, "Tribological behaviour of glass-ceramics reinforced by Yttria Stabilized Zirconia," *Tribology International,* vol. 102, pp. 361-370, 2016.

[22] J. A. Arsecularatne, J. P. Dingeldein, and M. Hoffman, "An in vitro study of the wear mechanism of a leucite glass dental ceramic," *Biosurface and Biotribology,* vol. 1, pp. 50-61, 2015.

[23] R. L. P. Santos, M. Bucimeaunu, F. S. Silva, J. C. M. Souza, R. M. Nascimento, F. V. Motta and B. Henriques, "Tribological behavior of zirconia-reinforced glass-ceramic composites in artificial saliva," *Tribology International,* vol. 103, pp. 379-387, 2016.

[24] ISO 6872 Dentistry-Ceramic materials. (2015). Switzerland.

[25] L. Wang, Y. Liu, W. Si, H. Feng, Y. Tao, and Z. Ma, "Friction and wear behaviors of dental ceramics against natural tooth enamel," Journal *of the European Ceramic Society,* vol. 32, pp. 2599-2606, 2012.